

Long-period Pulsars as Evidence of Supernova Fallback Accretion

M. RONCHI ^{1,2} N. REA ^{1,2} V. GRABER ^{1,2} AND N. HURLEY-WALKER ³

¹*Institute of Space Sciences (ICE, CSIC), Campus UAB, Carrer de Can Magrans s/n, E-08193, Barcelona, Spain*

²*Institut d'Estudis Espacials de Catalunya (IEEC), Carrer Gran Capità 2-4, E-08034 Barcelona, Spain*

³*International Centre for Radio Astronomy Research, Curtin University, Kent St, Bentley WA 6102, Australia*

Submitted to ApJ

ABSTRACT

For about half a century the radio pulsar population was observed to spin in the ~ 0.002 –12 s range, with different pulsar classes having spin-period evolution that differs substantially depending on their magnetic fields or past accretion history. The recent detection of several slowly rotating pulsars has re-opened the long-standing question of the exact physics, and observational biases, driving the upper bound of the period range of the pulsar population. In this work, we study the spin-period evolution of pulsars interacting with supernova fallback matter and specifically look at the fallback accretion disk scenario using general assumption for the pulsar spin period and magnetic field at birth, as well as fallback accretion rates. We show that this evolution can differ substantially from the typical dipolar spin-down, and can be very dependent on the ranges of initial parameters at formation, resulting in pulsars that show spin periods longer than their coeval peers. In addition, we study the case of the recently discovered radio transient GLEAM-X J162759.5-523504.3 ($P = 1091$ s). Long-period isolated pulsars might be more common than expected, being the natural result of supernova fallback accretion, and necessarily having a strong magnetic field.

1. INTRODUCTION

The spin-period distribution of the pulsar population reflects intrinsic properties of neutron star formation, early evolution, magnetic field decay, and age. Until a few years ago, the spin distribution of observed isolated pulsars was ranging between ~ 0.002 –12 s. At the fastest extreme, we have recycled millisecond pulsars (mostly in binaries), while the slowest extreme is populated by magnetars. The historical lack of isolated pulsars with periods $\gtrsim 12$ s has been intriguing and interpreted in different ways, ranging from the presence of a death line below which radio emission is quenched (Ruderman & Sutherland 1975; Bhattacharya & van den Heuvel 1991; Chen & Ruderman 1993), to magnetic field decay coupled with the presence of a highly resistive layer in the inner crust (possibly due to the existence of a nuclear pasta phase; Pons et al. 2013), as well as due to an observational bias caused by high band pass filters in radio searches (albeit not in the X-ray searches). Although the main reason is uncertain, all of these effects likely contribute at some level to the observational paucity of long-period pulsars (Wu et al. 2020).

However, recent radio surveys, in particular thanks to new radio interferometers such as LOw Frequency ARray (LO-

FAR; van Haarlem et al. 2013), MeerKAT (Jonas 2009), Australian SKA Pathfinder (ASKAP; Hotan et al. 2021), and Murchison Widefield Array (MWA; Tingay et al. 2013; Wayth et al. 2018), have started to uncover the existence of a new population of slowly rotating radio pulsars that challenge our understanding of the pulsar population and its evolution.

Two radio pulsars, PSR J1903+0433 (Han et al. 2021) and PSR J0250+5854 (Tan et al. 2018), have been recently discovered with periods of 14 s and 23 s, respectively. Moreover, a peculiar radio transient with a periodicity of ~ 1091 s (GLEAM-X J162759.5-523504.3; Hurley-Walker et al. 2022) have been discovered. This latter source has a very variable flux, showing periods of “radio outburst” lasting a few months, a 90% linear polarization, and a very spiky and variable pulse profile: characteristics typical for radio magnetars (Kaspi & Beloborodov 2017; Esposito et al. 2020) (although its magnetic field is still poorly constrained). Furthermore, a few years ago the X-ray emitting neutron star (1E 161348-5055) at the center of the 2 kyr old supernova remnant (SNR) RCW103, with a measured modulation of ~ 6.67 hr, showed a large magnetar-like X-ray outburst (Rea et al. 2016; D’Ai et al. 2016), demonstrating the source’s isolated magnetar nature despite its long period and young age.

To understand the origin of these slowly rotating neutron stars, we focus on the early stages of neutron star evolution following the core collapse supernova. Soon after their formation, neutron stars will necessarily witness fallback accre-

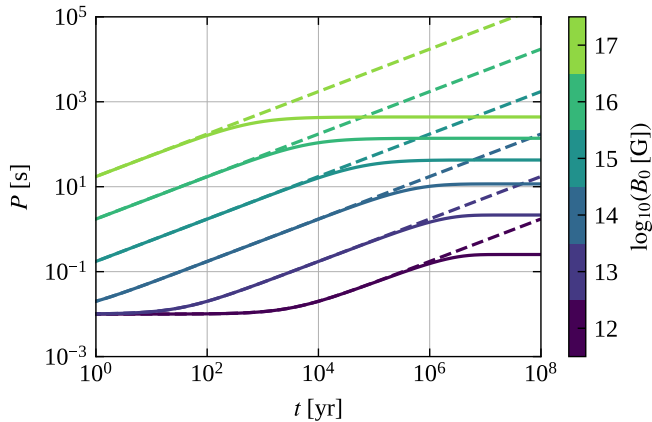


Figure 1. Spin-period evolution in time for dipolar spin down for different values of the initial magnetic field B_0 . The dashed lines represent the evolution curves for a constant magnetic field, while the solid lines represent the evolution tracks for a decaying magnetic field according to eq. 3.

tion with different accretion rates depending on the progenitor properties and explosion dynamics (Ugliano et al. 2012; Perna et al. 2014; Janka et al. 2021). If the fallback mass possesses sufficient angular momentum, it could form a long lasting accretion disk that will interact with the neutron star. For certain ranges of the initial spin period P_0 , magnetic field B_0 and disk accretion rate $\dot{M}_{d,0}$, fallback after the supernova explosion can substantially affect the pulsar spin evolution, in some cases slowing down the pulsar period significantly more than standard dipolar spin-down losses alone.

In this work, we specifically study the spin-period evolution of newly born pulsars that witness accretion from a fallback disk (§3), and determine the parameter ranges that allow pulsars to experience efficient spin-down. Furthermore, we study the characteristics of a newly discovered long-period transient radio source GLEAM-X J1627 (see §4) possibly interpreted as a long-period pulsar, to constrain its nature and evolution

(see §5). We provide a summary in §6.

2. PERIOD EVOLUTION OF PULSARS SLOWING DOWN VIA DIPOLAR LOSSES

Ordinary rotation powered pulsars are expected to slow down via electromagnetic dipolar losses, with an additional component driven by their magnetic field decay. In this scenario, if $\omega = 2\pi/P$ is the angular spin frequency of the pulsar, the electromagnetic torque causes the star to slow down according to:

$$\frac{d\omega}{dt} = -\beta B(t)^2 \omega^3, \quad (1)$$

where c is the speed of light and for an aligned rotator $\beta \sim R_{\text{NS}}^6 / (4c^3 I_{\text{NS}}) \sim 1.5 \times 10^{-41} \text{ s G}^{-2}$ assuming a typical neutron star radius $R_{\text{NS}} \sim 11 \text{ km}$, and moment of inertia $I_{\text{NS}} \sim 1.5 \times 10^{45} \text{ g cm}^2$. The inclination angle dependence

and uncertainty on the neutron star mass and radius introduce a correction of at most an order of magnitude to the value of β in the equation above (see for example Spitkovsky 2006).

If we consider a constant magnetic field $B(t) = B_0$, we can solve eq. (1) to find the spin-period evolution in time:

$$P(t) = P_0 \left(1 + \frac{8\pi^2 \beta B_0^2}{P_0^2} t \right)^{1/2}. \quad (2)$$

However, several studies have shown that neutron star magnetic fields evolve over time and decay due to the combined action of Ohmic dissipation and the Hall effect in the star's crust (Pons & Geppert 2007; Pons et al. 2009; Viganò et al. 2013; Pons & Viganò 2019; De Grandis et al. 2020). For simplicity, if we consider a crustal-confined magnetic field, we can use the phenomenological description of the field decay presented in Aguilera et al. (2008a,b), given by the analytic expression:

$$B(t) = B_0 \frac{e^{-t/\tau_{\text{Ohm}}}}{1 + \frac{\tau_{\text{Ohm}}}{\tau_{\text{Hall},0}} [1 - e^{-t/\tau_{\text{Ohm}}}]}. \quad (3)$$

This equation captures a first stage that is characterized by rapid (non-exponential) decay and regulated by the Hall timescale $\tau_{\text{Hall},0}$, and a second stage that is characterized by exponential decay due to Ohmic dissipation and regulated by the timescale τ_{Ohm} . These two characteristic timescales are defined by the following expressions:

$$\begin{aligned} \tau_{\text{Hall},0} &= \frac{4\pi e n_e L^2}{c B_0} \\ &\simeq 6.4 \times 10^5 \text{ yr} \left(\frac{n_e}{10^{36} \text{ cm}^{-3}} \right) \left(\frac{L}{1 \text{ km}} \right)^2 \left(\frac{B_0}{10^{14} \text{ G}} \right)^{-1}, \end{aligned} \quad (4)$$

$$\begin{aligned} \tau_{\text{Ohm}} &= \frac{4\pi \sigma L^2}{c^2} \\ &\simeq 4.4 \times 10^6 \text{ yr} \left(\frac{\sigma}{10^{24} \text{ s}^{-1}} \right) \left(\frac{L}{1 \text{ km}} \right)^2, \end{aligned} \quad (5)$$

where e is the electron charge, n_e is an average electron density in the neutron star crust, σ is the dominant conductivity based on phonon or impurity scattering and L is the typical lengthscale over which the relevant physical quantities (i.e., n_e , B_0 and σ) change inside the crust (see Cumming et al. 2004; Gourgouliatos & Cumming 2014). Note also that in eq. (3), $\tau_{\text{Hall},0}$ represents the Hall timescale for the initial magnetic field strength B_0 (we refer to Aguilera et al. 2008b, for more details).

Using these prescriptions for the magnetic field, we solve eq. (1) and determine the evolution of the spin-period in time. In Fig. 1, we present the corresponding behaviour for B_0 values in the range 10^{12-17} G . We fix P_0 to a fiducial value of 10 ms. After an initial phase of duration $t_{\text{em}} \sim 8\pi^2 \beta B_0^2 / P_0^2$, where the spin period remains almost constant and equal to its initial value, P starts to evolve $\propto t^{1/2}$. If the magnetic

field remains constant, this evolution proceeds indefinitely (dashed lines). If B decays over time according to eq. 3, the electromagnetic torque eventually becomes negligible and the spin period stops increasing and stabilizes (solid lines). We also note that for $t \gg t_{\text{em}}$ the spin-period evolution becomes completely insensitive to the initial value P_0 .

From this plot it is evident that if one assumes a decaying, crust-dominated magnetic field, in order to explain the existence of rather young (age $\lesssim 10^6$ yr), slowly rotating neutron stars ($P \gtrsim 10$ s), one would require extreme values of their magnetic field strength ($B \gtrsim 10^{15}$ G). If instead the currents are predominantly present in the neutron star core, the magnetic field could stay stable and barely decay over time (see for example Viganò et al. 2021). This would allow the star to reach longer spin periods more easily, since a strong electromagnetic torque is maintained over longer times. As little is known about magnetic field evolution in neutron star cores (in particular the effect of superfluid and superconducting components on field evolution; Graber et al. 2015; Passamonti et al. 2017; Ofengeim & Gusakov 2018; Gusakov et al. 2020), we cannot exclude the possibility that long-period pulsars are the result only of electromagnetic spin down in the presence of strong and persistent, core-dominated magnetic fields, even if these conditions are unlikely. Instead, we argue below that these sources can be naturally explained in a different scenario, whose ingredients are readily available in standard neutron-star formation models.

3. PERIOD EVOLUTION OF PULSARS WITNESSING SUPERNOVA FALLBACK

An alternative scenario that could explain the existence of strongly magnetized and slowly rotating pulsars involves the interaction between a newly born highly magnetic neutron star and fallback material from the supernova explosion. In the following for simplicity, we assume that the star's magnetic field is crust-dominated and decays in time according to eq. (3). In the early stages after the supernova explosion, the proto-neutron star emits a powerful neutrino wind which exerts a pressure on the outer envelope of the progenitor star. The duration of this wind is believed to be of the order of ~ 10 s after core bounce, which corresponds to the neutrino-cooling timescale for a newborn neutron star (Ugliano et al. 2012; Ertl et al. 2016). On this timescale, the magnetosphere of the neutron star reaches an equilibrium configuration in the region swept by the neutrino wind. After the subsiding of this neutrino-driven wind, the gas in the inner envelopes of the exploding star decelerates due to the gravitational pull of the neutron star and collapses back. This leads to the onset of fallback accretion. According to simulations (Ugliano et al. 2012; Ertl et al. 2016; Janka et al. 2021), the total fallback mass can reach values up to $M_{\text{fb}} \lesssim 0.1 M_{\odot}$, while the fallback mass rate can reach values of around $\sim 10^{27-31} \text{ g s}^{-1}$ in the first $\sim 10 - 100$ s after bounce, afterwards decreasing according to a power law $\sim t^{-5/3}$, which is compatible with theoretical predictions for a spherical supernova fallback (Michel 1988; Chevalier 1989). However, if part of the fallback matter possesses sufficient angular momentum,

it will circularize to form an accretion disk. Hereafter, we will study in detail the case where a disk forms successfully and interacts with the central neutron star. At the end of this section, we briefly discuss the case where the conditions to form a disk are not met and fallback is expected to proceed almost spherically.

3.1. Accretion from a fallback disk

Mineshige et al. (1997); Menou et al. (2001) have studied the formation and time evolution of fallback accretion disks around compact objects. In particular, by using the self-similar solution of Cannizzo et al. (1990), Menou et al. (2001) found that the fallback material with excess angular momentum circularizes to form a disk on a typical viscous timescale $t_{\text{v}} \sim 2000$ s. This timescale determines the duration of an initial transient accretion phase characterized by a nearly constant accretion rate. Afterwards, as the supply of fallback matter decreases, the accretion rate in the disk declines itself as a power law. We follow these prescriptions and model the long-term time evolution of the accretion rate in the disk as:

$$\dot{M}_{\text{d}}(t) = \dot{M}_{\text{d},0} \left(1 + \frac{t}{t_{\text{v}}}\right)^{-\alpha}, \quad (6)$$

where $\alpha = 19/16 = 1.18$ if the disk opacity is dominated by electron scattering or $\alpha = 1.25$ if the disk is dominated by Kramer's opacity (Menou et al. 2001; Cannizzo et al. 1990). In the following, we adopt an intermediate value of $\alpha = 1.2$. In general determining the fraction of fallback matter finishing to form the disk is not trivial, since it depends on the progenitor star properties and on the supernova mechanism itself. Here we consider a broad range of values for the disk accretion rate between $10^{19-29} \text{ g s}^{-1}$ that is compatible with the disk accreting at a fraction of the overall supernova fallback rate as well as having a fraction of the total fallback mass M_{fb} . For a radiatively efficient disk, if this flow of matter is maintained constant throughout the disk up to the inner disk radius r_{in} , such accretion rates would result in luminosities up to $L_{\text{acc}} \simeq GM_{\text{NS}}\dot{M}_{\text{d}}/(2r_{\text{in}}) \simeq 10^{46} \text{ erg s}^{-1}$ for fiducial values $M_{\text{NS}} = 1.4M_{\odot}$, $\dot{M}_{\text{d}} = 10^{28} \text{ g s}^{-1}$ and $r_{\text{in}} = 10^8 \text{ cm}$; G is the gravitational constant. These luminosities far exceed the Eddington limit given by $L_{\text{Edd}} = 1.3 \times 10^{38} (M_{\text{NS}}/M_{\odot}) \text{ erg s}^{-1} \simeq 1.8 \times 10^{38} \text{ erg s}^{-1}$. It is thus expected that such super-critical inflows of matter produce winds and outflows that reduce the accretion rate in the inner disk region to values below the Eddington limit (Poutanen et al. 2007). In a simplified scenario, we hence assume that the accretion rate at the inner disk radius r_{in} has to be limited by the Eddington accretion rate, given by $\dot{M}_{\text{Edd}} \simeq 2L_{\text{Edd}}r_{\text{in}}/(GM_{\text{NS}}) \simeq 10^{18} (r_{\text{in}}/R_{\text{NS}}) \text{ g s}^{-1}$. Therefore, we model the accretion rate at r_{in} as:

$$\dot{M}_{\text{d},\text{in}} = \begin{cases} \dot{M}_{\text{Edd}} & \text{if } \dot{M}_{\text{d}} \geq \dot{M}_{\text{Edd}}, \\ \dot{M}_{\text{d}} & \text{if } \dot{M}_{\text{d}} < \dot{M}_{\text{Edd}}. \end{cases} \quad (7)$$

If this accretion rate is sufficiently high, the in-falling matter is able to deform and penetrate the closed magnetosphere whose boundary can be roughly defined by the light cylinder radius r_{lc} :

$$r_{lc} = \frac{c}{\omega}. \quad (8)$$

In this case, we define the magnetospheric radius r_m which represents the distance from the star where the magnetic pressure equals the ram pressure of the accreted flow (Davidson & Ostriker 1973; Elsner & Lamb 1977; Ghosh & Lamb 1979):

$$r_m = \xi \left(\frac{\mu^4}{2GM_{NS}M_{d,in}^2} \right)^{\frac{1}{7}}, \quad (9)$$

where $\xi \sim 0.5$ is a corrective factor that takes into account that the accretion disk has a non-spherical geometry (Long et al. 2005; Bessolaz et al. 2008; Zanni & Ferreira 2013), $\mu = B(t)R_{NS}^3/2$ is the stellar magnetic moment, and $B(t)$ is the time dependent magnetic field at the pole (assuming a dipolar structure for the magnetosphere). Inside this magnetospheric radius, the plasma dynamics are dominated by the magnetic field so that the accretion flow is forced to corotate with the star's closed magnetosphere. Under such conditions, the magnetospheric radius roughly determines the inner edge of the accretion disk so that we can assume $r_{in} \sim r_m$.

If the accretion rate is sufficiently low, the magnetic pressure of the closed magnetosphere is able to keep the accretion flow outside the light cylinder. However beyond r_{lc} , the dipole configuration breaks down, the magnetic field lines open up and as a consequence they are no longer able to exert significant pressure on the accreted plasma. Under these conditions, we expect the inner radius r_{in} of the disk to be roughly equal to r_{lc} . Thus, in general we adopt the same prescription as Yan et al. (2012) and assume $r_{in} \simeq \min(r_m, r_{lc})$.

Another critical lengthscale is the corotation radius r_{cor} , which represents the distance at which the gravitational pull of the neutron star balances the centrifugal force for a test mass that is corotating with the star at the spin frequency ω :

$$r_{cor} = \left(\frac{GM_{NS}}{\omega^2} \right)^{\frac{1}{3}}. \quad (10)$$

The position of the magnetospheric radius with respect to the other two radii determines the total torque N_{tot} exerted on the star, which in turn drives the time evolution of the spin period according to:

$$I_{NS}\dot{\omega} = N_{tot} = N_{acc} + N_{dip}, \quad (11)$$

where N_{dip} accounts for the electromagnetic torque of the magnetosphere and N_{acc} accounts for the torque exerted by

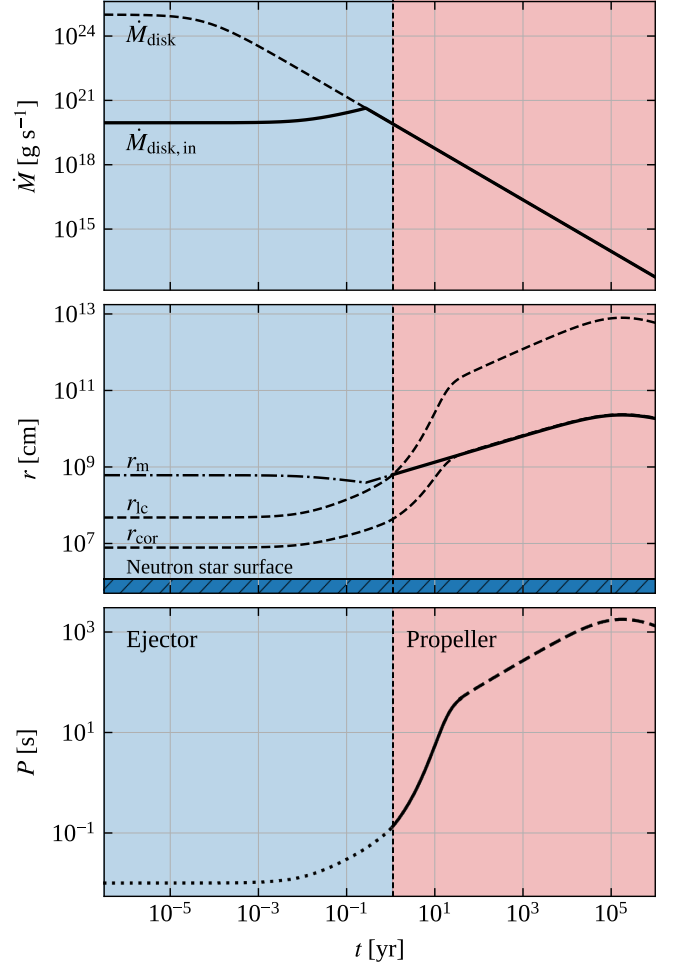


Figure 2. Pulsar spin-down in presence of a fallback disk. The top panel shows the total disk accretion \dot{M}_d and the Eddington-limited accretion rate at the inner radius $\dot{M}_{d,in}$. The middle panel illustrates the evolution of the three critical radii r_{cor} , r_m , r_{lc} . The bottom panel shows the resulting time evolution of the spin period. We assume an initial spin period $P_0 = 10$ ms, initial magnetic field $B_0 = 5 \times 10^{14}$ G and an initial disk accretion rate $\dot{M}_{d,0} = 10^{25}$ g s $^{-1}$. We also highlight the duration of the ejector and propeller phases by shading the background in blue and red, respectively.

the accretion process. Following Piro & Ott (2011); Metzger et al. (2018) the total torque can be modeled by the following equation:

$$N_{tot} = \begin{cases} \dot{M}_{d,in} r_{lc}^2 [\Omega_K(r_{lc}) - \omega] \\ \quad - I_{NS} \beta B^2 \omega^3 & \text{if } r_m > r_{lc}, \\ \dot{M}_{d,in} r_m^2 [\Omega_K(r_m) - \omega] \\ \quad - I_{NS} \left(\frac{r_{lc}}{r_m} \right)^2 \beta B^2 \omega^3 & \text{if } r_m \leq r_{lc}. \end{cases} \quad (12)$$

Fig. 2 shows an example of a solution of eq. (11) for a pulsar interacting with a fallback disk. We consider an initial

spin period $P_0 = 10$ ms, initial magnetic field $B_0 = 5 \times 10^{14}$ G and an initial disk accretion rate $\dot{M}_{d,0} = 10^{25}$ g s $^{-1}$.

Regarding the accretion torque N_{acc} , i.e. the first term in eq. (12), different regimes are present depending on the relative ordering of the three radii defined above. In particular with reference to Fig. 2, we distinguish:

- For $r_m > r_{lc} > r_{cor}$, the accreted material remains at the boundary of the closed magnetosphere and does not influence the neutron star's internal dynamics; i.e., the star spins down mainly due to dipolar electromagnetic torques. This phase is commonly referred to as ejector phase (shaded blue region in Fig. 2). The mechanism responsible for radio emission can be active and the neutron star could be observed as a radio pulsar.
- For $r_{lc} > r_m > r_{cor}$, the accretion flow is able to penetrate inside the closed magnetosphere. As it reaches the magnetospheric radius, the plasma flow is forced to corotate with the magnetosphere at super-Keplerian speeds causing it to be ejected due to centrifugal forces. This introduces a viscous torque that spins down the star very efficiently; a phase commonly referred to as the propeller (shaded red region in Fig. 2). In this case, we have $\omega > \Omega_K(r_m)$, where $\Omega_K(r) = (GM_{NS}/r^3)^{1/2}$ is the Keplerian orbital angular velocity at radius r . During this propeller phase, the spin frequency decreases over time and as $\omega \sim \Omega_K(r_m)$ (i.e., when $r_{cor} \sim r_m$), the net torque exerted on the neutron star vanishes so that it evolves towards spin equilibrium. From this point onward, further evolution of the spin period will be regulated mainly by time variation of the accretion rate at the inner radius of the disk $\dot{M}_{d,in}$ and the stellar magnetic field B . For example, the decay of the magnetic field strength causes the slow decrease of the magnetospheric radius at late times. This drives a progressive shift of the spin-equilibrium radius towards the neutron star surface, causing the neutron star to slightly spin up; in the example in Fig. 2, this happens at $\sim 10^5$ yr.
- For $r_{lc} > r_{cor} > r_m$, we have $\omega < \Omega_K(r_m)$. The accretion flow still manages to penetrate inside the closed magnetosphere but as it reaches the magnetospheric radius, the plasma is forced to corotate with the magnetosphere at sub-Keplerian speeds. In other words, at the boundary defined by the magnetospheric radius, the accreted plasma is orbiting faster than the neutron star magnetosphere. This introduces a viscous torque that transfers angular momentum from the plasma flow to the star causing it to spin up. In the example in Fig. 2, this phase is never experienced.

The electromagnetic torque N_{dip} , i.e., the second term in eq. (12), is also influenced by the accretion regime. When the accretion flow penetrates inside the closed magnetosphere, a fraction of the magnetic field lines, which connects the star

to the disk, is forced to open and as a consequence the polar cap region with open field lines expands, enhancing the spin-down torque caused by the magnetosphere (Parfrey et al. 2016; Metzger et al. 2018). In particular Parfrey et al. (2016) argue that for $r_m < r_{lc}$, the magnetic flux through the expanded polar cap increases by a factor $\sim (r_{lc}/r_m)$. As a consequence, since the dipole spin-down torque is proportional to the square of the magnetic flux through the open field-line region, N_{dip} is enhanced by a factor $\sim (r_{lc}/r_m)^2$. Moreover, since the radio emission is believed to be associated with magnetospheric currents and pair production (Beloborodov 2008; Philippov et al. 2020), as the closed-magnetosphere geometry is disturbed by the accretion flow, the mechanism believed to generate the radio emission could be perturbed or even stopped, effectively switching off the radio-loud nature of these sources (Li 2006).

From these considerations, we observe that the parameters that mainly regulate the evolution of a pulsar surrounded by a fallback disk are the initial stellar magnetic field B_0 and the initial disk accretion rate $\dot{M}_{d,0}$. The latter determines the time at which the accretion rate affecting the compact object becomes sub-Eddington and starts decreasing. In contrast, the value of the neutron star's initial spin period only affects the early evolution stages, while the long-term evolution of the neutron star is almost insensitive to the value of P_0 .

Fig. 3 and 4 show several examples of evolutionary curves of the spin period. We always assume an initial spin period $P_0 = 10$ ms. In particular, Fig. 3 shows the spin-period evolution for several values of the initial magnetic field B_0 and varying initial disk accretion rate $\dot{M}_{d,0}$, while Fig. 4 shows the evolution curves for several values of initial disk accretion rate and varying initial magnetic field. In the early phases, the accretion at the inner radius of the disk is limited by the Eddington limit. For low values of the magnetic field ($\lesssim 10^{12}$ G), the magnetospheric radius falls within the closed magnetosphere and the neutron star starts its life in propeller (solid portion of the curves). As time advances, it can either remain in propeller if $\dot{M}_{d,0}$ is high enough or it can shift to an ejector state for lower values of $\dot{M}_{d,0}$ (dotted portion of the curves). On the other end, for sufficiently high magnetic field values ($> 10^{12}$ G), the magnetospheric radius falls outside of the closed magnetosphere. Under these conditions, the star starts its life in the ejector phase. However, as \dot{M}_d decreases and eventually becomes sub-Eddington, since in the ejector phase the light cylinder radius evolves faster in time ($\propto t^{1/2}$) than the magnetospheric radius ($\propto t^{2\alpha/7} \simeq t^{0.34}$ for $\alpha = 1.2$), the star shifts to the propeller phase causing significant spin down. Note that the higher the initial magnetic field B_0 and the initial disk accretion rate $\dot{M}_{d,0}$, the earlier the neutron star enters the propeller regime. Finally, as the corotation radius approaches the magnetospheric radius, the neutron star stabilizes in a spin equilibrium (dashed portion of the curves). Note also that, especially for the highest magnetic field strengths, the effect of field decay is visible in the turn over of the evolutionary curves at times $\gtrsim 10^4$ yr.

We note that a neutron star that enters the propeller phase and subsequently reaches spin equilibrium will remain in this

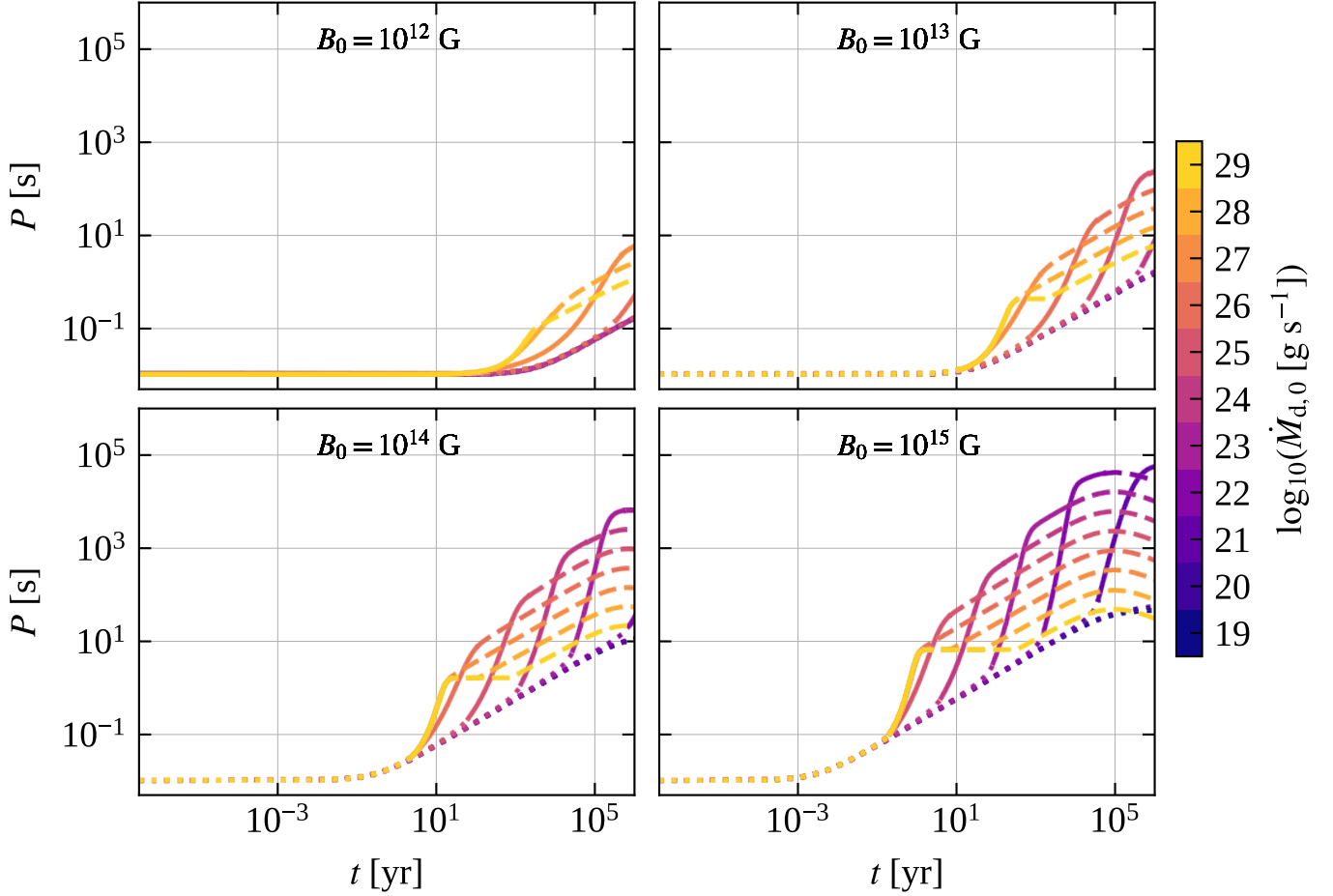


Figure 3. Example curves showing the time evolution of the spin period for a pulsar interacting with a fallback disk for different assumptions on the initial B_0 field strength, and varying disk fallback rate $\dot{M}_{d,0}$. The dotted portion of the curves indicates when the neutron star is in the radio-loud ejector phase, i.e., when $r_m > r_{lc}$, while the solid portion indicates when the neutron star is in the radio-quiet propeller stage, i.e., when $r_{cor} < r_m < r_{lc}$. The dashed lines highlight when the neutron star has reached spin equilibrium.

state until an abrupt change in the disk accretion rate occurs. For example if the accretion rate in the disk suddenly drops, a neutron star can exit the propeller phase and enter the ejector phase again. In this case, the neutron star can transition from a faint X-ray source (due to thermal emission from material accreted onto the magnetosphere) to a standard rotation-powered radio pulsar or potentially radio-loud magnetar (see §5 for a detailed explanation of how this transition can occur and a description of the expected X-ray and radio luminosity in the different fall-back accretion states).

3.2. Accretion from spherical fall-back

If the fallback matter does not possess sufficient angular momentum to form a disk, fallback will proceed quasi-spherically. Even in this case, the neutron star could experience different accretion phases depending on the magnitude of the fallback rate. If the matter inflow is radiatively inefficient, accretion could proceed at super-Eddington rates, especially in the early stages. For such high fallback rates, the accretion flow is likely able to penetrate and squeeze the proto-neutron star magnetosphere, causing an initial phase of

direct accretion onto the surface. This might also result in the burial of the magnetic field (see for example Taam & van den Heuvel 1986; Li et al. 2021; Lin et al. 2021), a scenario that (combined with the subsequent secular re-emergence of the magnetic field) has been invoked to explain the observed properties of Central Compact Objects (CCOs) (Halpern & Gotthelf 2010; Fu & Li 2013; Ho 2015; Zhong et al. 2021); a class of young, generally weak-field neutron stars found close to the centers of supernova remnants. After this initial direct accretion phase, as the fallback rate decreases in time, the neutron star could enter a propeller phase that could cause the star to spin-down as in the disk scenario. However in the case of quasi-spherical accretion, the fallback episode is expected to last at most a free-fall timescale $t_{ff} \sim (G\rho)^{-1/2}$ determined by the density ρ of the infalling stellar outer layers participating in the fallback. In general t_{ff} reaches at most $\sim 10^7$ s for red supergiant progenitor stars (Metzger et al. 2018). Therefore, it is unlikely that a propeller phase acting on such short timescales (of the order of ~ 1 yr) could result in equally long spin periods as the disk scenario.

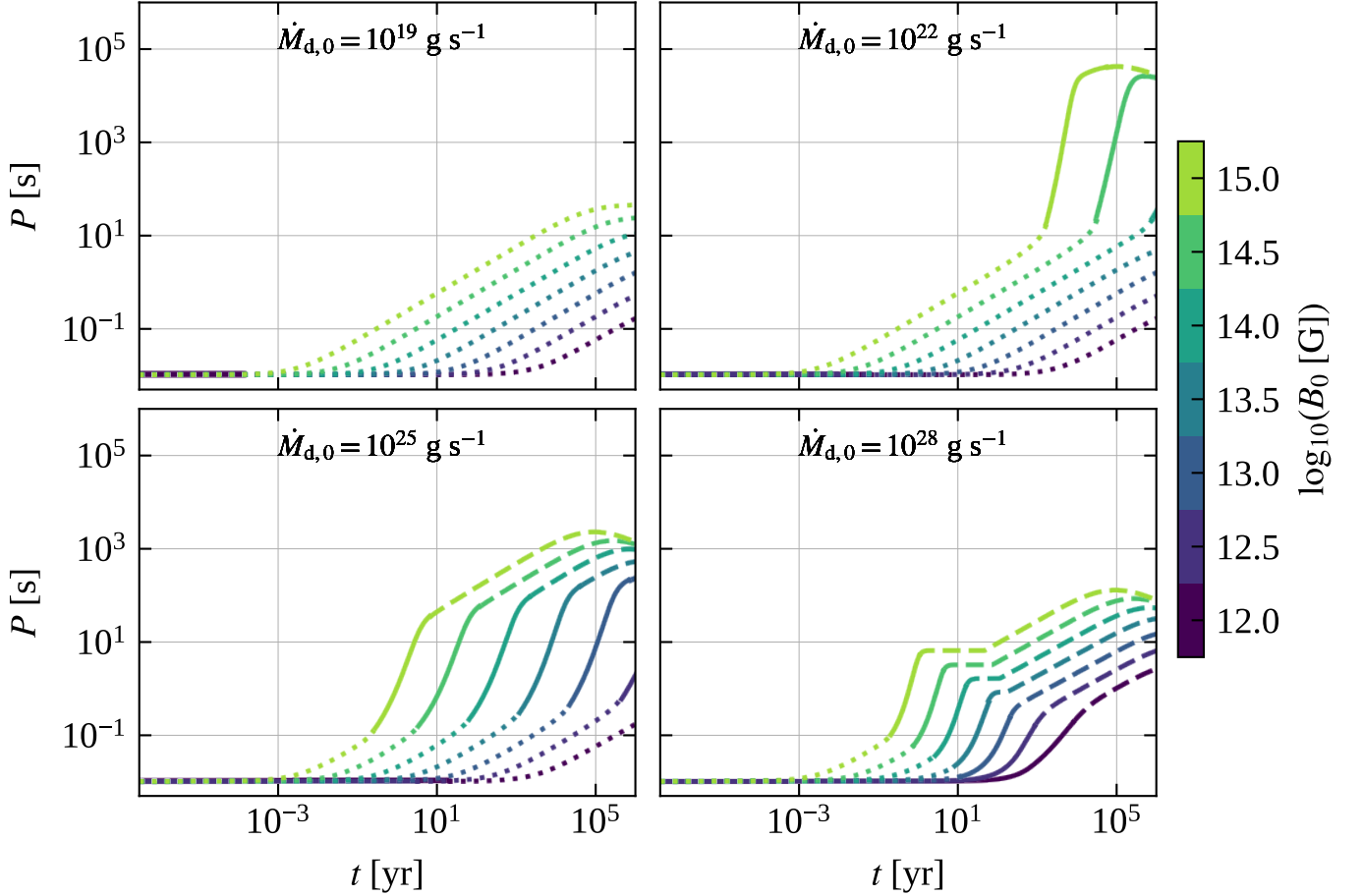


Figure 4. Example curves showing the time evolution of the spin period for a pulsar interacting with a fallback disk for different assumptions of the disk fallback rate $\dot{M}_{d,0}$, and varying the initial magnetic field B_0 . The dotted portion of the curves indicate when the neutron star is in the radio-loud ejector phase, i.e., when $r_m > r_{lc}$, while the solid portion indicates when the neutron star is in the radio-quiet propeller stage, i.e., when $r_{cor} < r_m < r_{lc}$. The dashed lines highlight when the neutron star has reached spin equilibrium.

4. THE 18 MIN PERIODIC RADIO TRANSIENT GLEAM-X J162759.5-523504.3

During the GaLactic and Extragalactic All-sky MWA eXtended survey (GLEAM-X) (Hurley-Walker et al. in prep.) with the Murchison Widefield Array (MWA), a peculiar periodic radio transient has been discovered displaying a periodicity of 1091 s (Hurley-Walker et al. 2022). The source was detected during two radio outburst periods in January and March 2018, displaying a very variable flux (going from undetected to values as high as 20–50 Jy), $\sim 5\%$ duty cycle, 90% linear polarization, and a very spiky and variable pulse profile.

From a detailed timing analysis, a dispersion measure of $DM = 57 \pm 1 \text{ pc cm}^{-3}$ was calculated, converting to a distance of 1.3 kpc according to the Galactic electron-density model of Yao et al. (2017). The period derivative was loosely constrained to $\dot{P} < 1.5 \times 10^{-9} \text{ s s}^{-1}$. Assuming that the source is an isolated neutron star spinning down due to the classical electromagnetic dipole formula, this gives a relatively weak constraint on the dipolar magnetic field of $B_{\text{dip}} < 10^{17} \text{ G}$. We can also obtain an upper limit on the

spin-down power $\dot{E}_{\text{rot}} = I_{\text{NS}} \omega \dot{\omega} < 10^{28} \text{ erg s}^{-1}$. If we roughly estimate an isotropic radio luminosity from the flux detected during the outburst phase and the distance estimated from the DM, we obtain a value of $\sim 10^{31} \text{ erg s}^{-1}$. From this, we deduce that the spin-down alone is insufficient to power these very bright radio flares. The radio characteristics, such as the large flux variability, the radio outburst activity, and the high linear polarization, seem indeed to be analogous to the ones observed in radio-active magnetars; although its exceptionally long spin period would make this source stand out among them.

As shown in Fig. 1, if we assume that GLEAM-X J1627 is indeed a magnetar that has spun down to a 1091 s period via dipolar losses alone, it could have an age $\gtrsim 10^{6-7} \text{ yr}$ and would be characterized by a rather extreme and long-lasting magnetic field of 10^{15-16} G . As argued in §2, sustaining such a strong magnetic field over this lifetime is difficult to reconcile with the models predicting magnetic field dissipation in the neutron star crust due to the Hall effect which is expected to cause a strong field decay on timescales of around 10^{4-5} yr . If its magnetic energy reservoir has de-

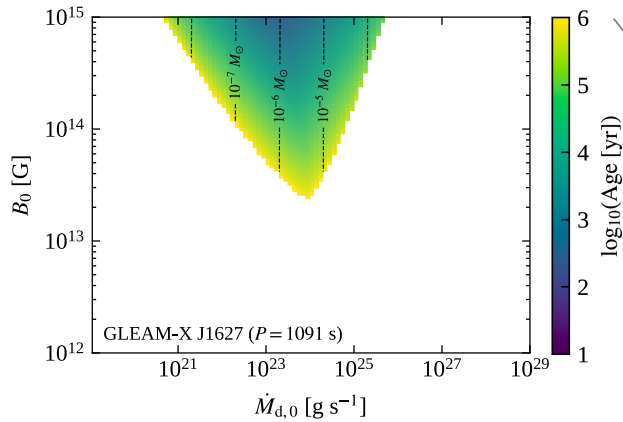


Figure 5. GLEAM-X J1627 in the supernova fallback-accretion picture. The colored region shows the values of the initial magnetic field B_0 and disk fallback rate $\dot{M}_{d,0}$ that allow the neutron star to reach a spin period of 1091 s in less than 10^6 yr. The color code indicates the time at which the possible neutron star has reached its period. The contour lines indicate the total fallback mass that has been accreted by the disk in the same time interval.

cayed in time, it becomes also challenging to explain the current magnetar-like activity observed from this source. Therefore, this scenario necessarily would require the presence of a strong and stable magnetic field in the neutron star core.

A more promising explanation for GLEAM-X J1627 that requires less extreme conditions is a magnetar that has experienced accretion from a fallback disk soon after the supernova. As outlined in §3, a magnetar surrounded by a fallback disk will pass through the propeller phase and spin down very efficiently on short timescales. To study this scenario for GLEAM-X J1627, we first fix the initial spin period to $P_0 = 10$ ms (remember that as long as $P \gg P_0$, P_0 has very little influence on the long-term evolution); for the neutron star mass and radius we adopt the fiducial values $M_{NS} = 1.4 M_\odot$ and $R_{NS} = 11$ km. By varying the two parameters B_0 and $\dot{M}_{d,0}$ and using eq. (12) to determine the torque acting on the star in the different stages, we can numerically integrate eq. (11) in time. This allows us to find those parameter combinations that lead to a spin-down evolution reaching a period of 1091 s. We assume that the pulsar is younger than 10^6 yr to be able to emit such powerful radio emission. Therefore, we truncate the evolution at this time.

Fig. 5 shows the parameter space of B_0 and $\dot{M}_{d,0}$, where we choose an initial magnetic field between 10^{12-15} G and an initial disk accretion rate between 10^{19-29} g s^{-1} . The colored region represents the combination of parameters that guarantees the neutron star to reach a spin period of 1091 s in less than 10^6 yr. The color code indicates the age at which the neutron star reaches the wanted period. The contour lines show the total fallback mass that has accreted into the disk over the same time interval (calculated by integrating eq. (6) in time). In this scenario, we observe that thanks to the propeller phase a magnetar with a magnetic field around 10^{14} G

can reach a spin period of 1091 s on the relatively short time scale of about 10^{4-5} yr, by considering a disk accretion rate of around $\dot{M}_{d,0} \sim 10^{24}$ g s^{-1} and a total accreted mass of around $\sim 10^{-5} M_\odot$.

5. DISCUSSION

5.1. Re-establishing the radio emission after the propeller

One key piece that we have to discuss is how a neutron star, that enters the propeller phase to experience effective spin-down, can exit this phase again in order to be observed as a radio-loud object; this is a crucial requirement, given that we wish to possibly explain the radio detection of GLEAM-X J1627. As briefly mentioned in §3, the transition from the propeller to the ejector phase can be naturally explained by an abrupt drop in the accretion rate. As a result, the magnetospheric radius would move beyond the light cylinder, providing the condition for the radio emission to be reactivated.

One possible explanation for a significant drop in the accretion flow could be simply that the fallback disk runs out of matter. During the propeller phase the material that reaches the magnetospheric radius is ejected due to the centrifugal barrier. If the ejected material passes a velocity superior to the escape velocity, it will become unbound from the system; otherwise it will fall back and be reprocessed inside the accretion disk. As the matter feeding the disk from the supernova fallback is not replenished, if the propeller is efficient at unbinding matter from the system, we expect the accretion disk to eventually be completely consumed (see for example Ekşi et al. 2005; Romanova et al. 2005).

Another possibility is that the fallback disk, which itself evolves with time, undergoes a thermal ionization instability. This instability, outlined in detail in Menou et al. (2001), occurs when the rate of fallback matter feeding the disk \dot{M}_d falls below a critical value of around $\sim 10^{16}$ g s^{-1} . When this occurs, the temperature in the disk decreases, starting from the outer disk regions. As the temperature drops below $\sim 10^4$ K, the recombination of free electrons with heavy nuclei in the plasma is triggered. The resulting recombination front rapidly propagates inwards and the disk becomes charge neutral. This transition alters the corresponding magnetic and viscous properties, causing the disk to no longer efficiently transfer angular momentum; as a result the accretion onto the neutron star is stopped. Menou et al. (2001) have shown that this transition occurs on a timescale of around 10^4 yr, which is compatible with the timescale we require in our fallback accretion scenario for neutron stars to reach spin periods > 10 s (see Fig. 5). The transition from the propeller to the ejector phase can thus be naturally explained if the disk becomes inactive and the accretion flow stops.

In Fig. 6, we show a possible evolutionary scenario for GLEAM-X J1627 that incorporates this drop in accretion rate. In particular, the top panel shows the spin-period evolution. For GLEAM-X J1627 we choose an initial disk accretion rate of $\dot{M}_{d,0} = 10^{24}$ g s^{-1} and an initial magnetic field $B_0 = 4 \times 10^{14}$ G. These values fall within the allowed parameter space that guarantees the two sources to reach their

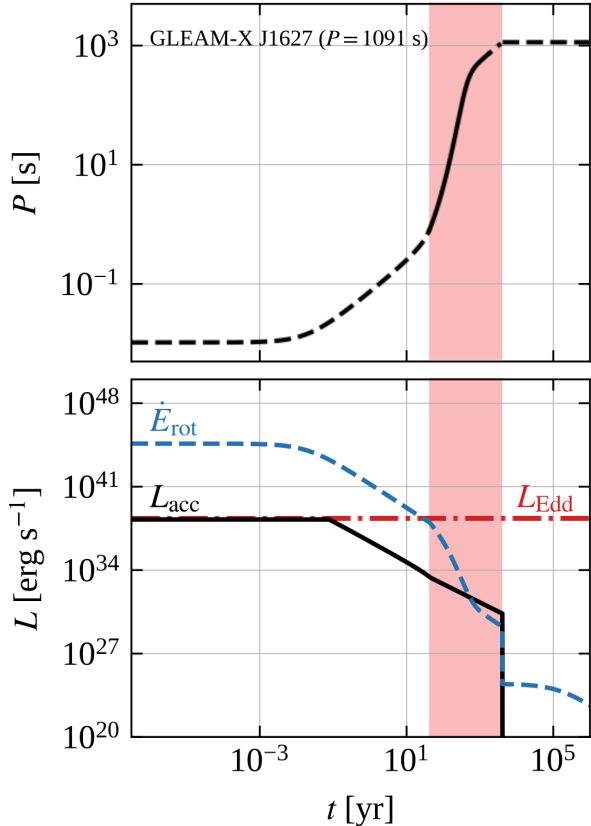


Figure 6. Example of the time evolution of the spin period (top panel), disk luminosity and spin-down power (bottom panel) for GLEAM-X J1627. We assume a magnetic field $B = 4 \times 10^{14}$ G and an initial disk accretion rate of $\dot{M}_{d,0} = 10^{24} \text{ g s}^{-1}$. The red shaded region indicates the interval during which the neutron star spin down in the propeller phase. We assume that after the pulsar have reached its observed period of 1091 s, an abrupt drop in accretion rate causes the recovery of the ejector phase.

spin period in less than 10^6 yr (see Fig. 5). To keep things simple, we set the disk accretion rate to zero as soon as the neutron star reach its observed spin period of 1091 s. This abrupt stop in the accretion process causes the source to transition into the ejector phase and enables the restoration of the radio emission.

On the other hand, if accretion persists, the neutron star continues to evolve in a spin-equilibrium, unable to exit the propeller phase. This is possibly the evolutionary phase currently witnessed for 1E 161348-5055, the 2 kyr old magnetar associated with the SNR RCW103. This source has shown magnetar-like outbursts (Rea et al. 2016; D’Ai et al. 2016) and an observed period of 6.67 hr but is detected only in the X-ray band. Its period evolution has been modeled by Ho & Andersson (2017) using a similar model to our own, albeit with a constant accretion flow. Using the more realistic prescription of time-varying accretion as discussed in §3, the

long period together with the young age of 1E 161348-5055 could be explained with a field of $\sim 10^{15}$ G (in line with the results of Ho & Andersson 2017) and a relatively low initial disk accretion rate of $\sim 10^{22} \text{ g s}^{-1}$ (see bottom right panel of Fig. 3 as a reference). As 1E 161348-5055 is currently not observed in radio, and thus still in the propeller phase, we infer that the accretion disk is still active, which is compatible with the source’s age of 2 kyr.

An association of long-period pulsars with supernova remnants could present additional proof for our fallback disk scenario. However, for GLEAM-X J1627 no clear evidence of SNR associations has been discovered so far. In general, SNRs are expected to have an observational lifetime of around 10^{4-5} yr (Braun et al. 1989; Leahy et al. 2020), which is comparable with our range of derived age for this source. It is therefore possible that the associated SNR is too faint to be detectable. Moreover, only one third of the known young pulsars have a detected SNR remnant. The reasons for this are still a matter of debate and study, but the absence of detected SNRs for most neutron stars could simply indicate differences in the progenitor, supernova explosion and interstellar environment (see for example Gaensler & Johnston 1995; Cui et al. 2021). We therefore do not consider the lack of SNR association as an issue for the validity of a fallback disk scenario.

5.2. Prediction for the X-ray and radio luminosity of long-period pulsars

In the bottom panel of Fig. 6, we show the evolution of the disk luminosity and spin-down power for GLEAM-X J1627. The accretion luminosity is computed as $L_{\text{acc}} \simeq GM_{\text{NS}}\dot{M}_d/(2r_{\text{in}})$, where we recall that $r_{\text{in}} \simeq \min(r_{\text{m}}, r_{\text{lc}})$. At very early times, i.e., $\lesssim 1$ yr after the supernova, the accretion flow is expected to be limited by the Eddington limit, suggesting that the disk emits in X-rays at the Eddington luminosity. As the system evolves and the disk accretion rate starts to decrease as $t^{-\alpha}$, the inner disk radius increases following the evolution of the magnetospheric radius as $r_{\text{in}} \sim r_{\text{m}} \propto t^{2\alpha/7}$. As a consequence, the luminosity decreases roughly as $\propto t^{-9\alpha/7}$. Once the disk becomes inactive or is completely consumed, the accretion rate is expected to vanish and the disk becomes undetectable in the X-rays. Therefore assuming the fallback scenario for long-period radio transients such as GLEAM-X J1627 with a ceasing of the accretion flow, X-ray observations should not be able to detect emission from a residual disk if present. The cold debris of an inactive disk could instead be detectable in the infrared (Wang et al. 2006). However, if the central neutron stars are indeed young (around 10^{4-5} yr) and have strong magnetic fields, they could emit thermal X-rays at their surfaces with luminosities up to $\sim 10^{30-35} \text{ erg s}^{-1}$ due to the dissipation of magnetic energy in the crust (Viganò et al. 2013).

In Fig. 6 we also show the evolution of the spin-down power that is typically taken as the energy source for the radio emission of pulsars. In general, after these neutron stars have exited the propeller phase and recovered the ejector regime, we expect the spin-down to be caused only by electromag-

netic torques so that $\dot{E}_{\text{rot}} \propto B^2/P^4$. Therefore, if we consider an upper limit for the magnetic field of around 10^{15} G and a lower limit for the spin periods after the propeller regime of around 10 s, for long-period pulsar we expect that the spin-down power has decayed to values $\lesssim 10^{33}$ erg s $^{-1}$. This energy budget together with the magnetic energy stored in their strong fields could be enough to power radio emission and cause magnetar-like activity for neutron stars of this kind.

6. SUMMARY

We have studied the spin evolution of young, isolated neutron stars under the influence of fallback disk accretion. We specifically focused on this scenario as a promising origin of long-period pulsars, a class of objects that have been discovered in recent radio surveys. By solving the torque balance equation for a disk accreting neutron star, we demonstrate that the evolution of such an object can significantly differ from standard dipole spin-down. In particular, we find that for a combination of high (but not extreme) magnetic fields strengths and moderate fallback disk accretion rates in agreement with current core-collapse supernova simulations, neutron stars can enter the propeller phase during their evolution. This leads to effective spin-down and allows neutron stars to reach spin periods $\gg 10$ s on time scales on the order of $\sim 10^{4-5}$ yr, which is unlikely via magnetic dipolar losses alone, unless extreme magnetic field values or a long-lasting core field component are invoked.

We have then studied the recently discovered object GLEAM-X J1627 (Hurley-Walker et al. 2022) with a periodic emission of 1091 s, in light of this model, and showed that if interpreted as a pulsar it is difficult to reconcile with dipolar losses alone; it would require extreme core-dominated magnetic fields to be maintained for long times. On the other hand, it can be easily explained as a highly magnetized neutron star with a fallback disk accretion history. The possibility to reach such long spin periods in much less than 10^6 yr is crucial to maintain the magnetic field and thus an energy reservoir to power their radio or X-ray activity. This is particularly important given that GLEAM-X J1627, was observed in outburst similar to other young radio-loud magnetars.

We showed that for newly born neutron stars with birth fields of $B_0 \sim 10^{14-15}$ G, a phase of fallback disk accretion can easily explain their detection as long-period radio or X-ray pulsars at relatively young ages ($\sim 10^{4-5}$ yr). On the other hand, in systems where the initial magnetic fields are lower ($\sim 10^{12-13}$ G), fallback disk accretion (even if present) is expected to have a negligible effect on the spin-period evolution on the timescales of $\sim 10^4$ yr. The major-

ity of neutron stars will therefore primarily undergo standard dipolar electromagnetic spin-down and recover rotation periods below ~ 12 s. In our framework, we therefore naturally recover the pulsar population which is observed to spin in the range $\sim 0.002-12$ s. Note that the recently discovered radio pulsars PSR J1903+0433 (Han et al. 2021) and PSR J0250+5854 (Tan et al. 2018) with periods of 14 s and 23 s, respectively, could be easily accommodated within our fallback accretion scenario. However, both sources can in principle also be explained within the standard evolutionary scenario provided that crustal field decay is very weak (essentially requiring the absence of a highly resistive pasta layer; see Pons et al. 2013) and/or a strong core magnetic field is present.

We also mentioned the X-ray emitting magnetar at the center of the 2 kyr old SNR RCW103, which requires (ongoing) fallback to explain its 6.67 hr period and radio-quiet nature. Finally note that classical magnetars with periods $\lesssim 12$ s would correspond to those systems where only strong fields are present, but fallback disk accretion does not take place or is inefficient because of a low $\dot{M}_{\text{d},0}$.

In conclusion, we have argued that fallback disk accretion is a common scenario after the supernova explosions of massive stars, and naturally expected to affect the evolution of the newly born neutron star. Depending on the relative intensities of the initial pulsar magnetic field and accretion rates, we can easily explain different neutron star classes and specifically the long-period objects discovered recently.

We are grateful to Rosalba Perna for insightful discussions on fossil disk accretion and physics, and Daniele Viganó for useful comments on this manuscript. We also thank Francesco Coti Zelati, Alice Borghese, José Pons and Clara Dehman for useful discussions. We apologize with M. Caleb and her team for having unintentionally released sensible information on their work in an earlier version of this manuscript. MR’s work has been carried out within the framework of the doctoral program in Physics of the Universitat Autònoma de Barcelona. MR, NR, and VG are supported by the H2020 ERC Consolidator Grant “MAGNESIA” under grant agreement No. 817661 (PI: Rea) and National Spanish grant PGC2018-095512-BI00. NHW is supported by an Australian Research Council Future Fellowship (project number FT190100231) funded by the Australian Government. This work was also partially supported by the program Unidad de Excelencia María de Maeztu CEX2020-001058-M, and by the PHAROS COST Action (No. CA16214).

REFERENCES

- Aguilera, D. N., Pons, J. A., & Miralles, J. A. 2008a, *ApJL*, 673, L167, doi: [10.1086/527547](https://doi.org/10.1086/527547)
- . 2008b, *A&A*, 486, 255, doi: [10.1051/0004-6361:20078786](https://doi.org/10.1051/0004-6361:20078786)
- Beloborodov, A. M. 2008, *ApJL*, 683, L41, doi: [10.1086/590079](https://doi.org/10.1086/590079)
- Bessolaz, N., Zanni, C., Ferreira, J., Keppens, R., & Bouvier, J. 2008, *A&A*, 478, 155, doi: [10.1051/0004-6361:20078328](https://doi.org/10.1051/0004-6361:20078328)

- Bhattacharya, D., & van den Heuvel, E. P. J. 1991, *PhR*, 203, 1, doi: [10.1016/0370-1573\(91\)90064-S](https://doi.org/10.1016/0370-1573(91)90064-S)
- Braun, R., Goss, W. M., & Lyne, A. G. 1989, *ApJ*, 340, 355, doi: [10.1086/167398](https://doi.org/10.1086/167398)
- Cannizzo, J. K., Lee, H. M., & Goodman, J. 1990, *ApJ*, 351, 38, doi: [10.1086/168442](https://doi.org/10.1086/168442)
- Chen, K., & Ruderman, M. 1993, *ApJ*, 402, 264, doi: [10.1086/172129](https://doi.org/10.1086/172129)
- Chevalier, R. A. 1989, *ApJ*, 346, 847, doi: [10.1086/168066](https://doi.org/10.1086/168066)
- Cui, X.-H., Zhang, C.-M., Li, D., et al. 2021, *MNRAS*, 508, 279, doi: [10.1093/mnras/stab2498](https://doi.org/10.1093/mnras/stab2498)
- Cumming, A., Arras, P., & Zweibel, E. 2004, *ApJ*, 609, 999, doi: [10.1086/421324](https://doi.org/10.1086/421324)
- D’Ai, A., Evans, P. A., Gehrels, N., et al. 2016, *The Astronomer’s Telegram*, 9180, 1
- Davidson, K., & Ostriker, J. P. 1973, *ApJ*, 179, 585, doi: [10.1086/151897](https://doi.org/10.1086/151897)
- De Grandis, D., Turolla, R., Wood, T. S., et al. 2020, *ApJ*, 903, 40, doi: [10.3847/1538-4357/abb6f9](https://doi.org/10.3847/1538-4357/abb6f9)
- Ekşi, K. Y., Hernquist, L., & Narayan, R. 2005, *ApJL*, 623, L41, doi: [10.1086/429915](https://doi.org/10.1086/429915)
- Elsner, R. F., & Lamb, F. K. 1977, *ApJ*, 215, 897, doi: [10.1086/155427](https://doi.org/10.1086/155427)
- Ertl, T., Ugliano, M., Janka, H.-T., Marek, A., & Arcones, A. 2016, *ApJ*, 821, 69, doi: [10.3847/0004-637X/821/1/69](https://doi.org/10.3847/0004-637X/821/1/69)
- Esposito, P., Rea, N., Borghese, A., et al. 2020, *ApJL*, 896, L30, doi: [10.3847/2041-8213/ab9742](https://doi.org/10.3847/2041-8213/ab9742)
- Fu, L., & Li, X.-D. 2013, *ApJ*, 775, 124, doi: [10.1088/0004-637X/775/2/124](https://doi.org/10.1088/0004-637X/775/2/124)
- Gaensler, B. M., & Johnston, S. 1995, *MNRAS*, 277, 1243, doi: [10.1093/mnras/277.4.1243](https://doi.org/10.1093/mnras/277.4.1243)
- Ghosh, P., & Lamb, F. K. 1979, *ApJ*, 232, 259, doi: [10.1086/157285](https://doi.org/10.1086/157285)
- Gourgouliatos, K. N., & Cumming, A. 2014, *MNRAS*, 438, 1618, doi: [10.1093/mnras/stt2300](https://doi.org/10.1093/mnras/stt2300)
- Graber, V., Andersson, N., Glampedakis, K., & Lander, S. K. 2015, *MNRAS*, 453, 671, doi: [10.1093/mnras/stv1648](https://doi.org/10.1093/mnras/stv1648)
- Gusakov, M. E., Kantor, E. M., & Ofengeim, D. D. 2020, *MNRAS*, 499, 4561, doi: [10.1093/mnras/staa3160](https://doi.org/10.1093/mnras/staa3160)
- Halpern, J. P., & Gotthelf, E. V. 2010, *ApJ*, 709, 436, doi: [10.1088/0004-637X/709/1/436](https://doi.org/10.1088/0004-637X/709/1/436)
- Han, J. L., Wang, C., Wang, P. F., et al. 2021, *Research in Astronomy and Astrophysics*, 21, 107, doi: [10.1088/1674-4527/21/5/107](https://doi.org/10.1088/1674-4527/21/5/107)
- Ho, W. C. G. 2015, *MNRAS*, 452, 845, doi: [10.1093/mnras/stv1339](https://doi.org/10.1093/mnras/stv1339)
- Ho, W. C. G., & Andersson, N. 2017, *MNRAS*, 464, L65, doi: [10.1093/mnras/slw186](https://doi.org/10.1093/mnras/slw186)
- Hotan, A. W., Bunton, J. D., Chippendale, A. P., et al. 2021, *PASA*, 38, e009, doi: [10.1017/pasa.2021.1](https://doi.org/10.1017/pasa.2021.1)
- Hurley-Walker, N., Zhang, X., Bahramian, A., et al. 2022, *Nature*, 601, 526, doi: [10.1038/s41586-021-04272-x](https://doi.org/10.1038/s41586-021-04272-x)
- Janka, H. T., Wongwathanarat, A., & Kramer, M. 2021, arXiv e-prints, arXiv:2104.07493. <https://arxiv.org/abs/2104.07493>
- Jonas, J. L. 2009, *IEEE Proceedings*, 97, 1522, doi: [10.1109/JPROC.2009.2020713](https://doi.org/10.1109/JPROC.2009.2020713)
- Kaspi, V. M., & Beloborodov, A. M. 2017, *ARA&A*, 55, 261, doi: [10.1146/annurev-astro-081915-023329](https://doi.org/10.1146/annurev-astro-081915-023329)
- Leahy, D. A., Ranasinghe, S., & Gelowitz, M. 2020, *ApJS*, 248, 16, doi: [10.3847/1538-4365/ab8bd9](https://doi.org/10.3847/1538-4365/ab8bd9)
- Li, S.-Z., Yu, Y.-W., Gao, H., & Zhang, B. 2021, *ApJ*, 907, 87, doi: [10.3847/1538-4357/abcc70](https://doi.org/10.3847/1538-4357/abcc70)
- Li, X.-D. 2006, *ApJL*, 646, L139, doi: [10.1086/506962](https://doi.org/10.1086/506962)
- Lin, W., Wang, X., Wang, L., & Dai, Z. 2021, *ApJL*, 914, L2, doi: [10.3847/2041-8213/ac004a](https://doi.org/10.3847/2041-8213/ac004a)
- Long, M., Romanova, M. M., & Lovelace, R. V. E. 2005, *ApJ*, 634, 1214, doi: [10.1086/497000](https://doi.org/10.1086/497000)
- Menou, K., Perna, R., & Hernquist, L. 2001, *ApJ*, 559, 1032, doi: [10.1086/322418](https://doi.org/10.1086/322418)
- Metzger, B. D., Beniamini, P., & Giannios, D. 2018, *ApJ*, 857, 95, doi: [10.3847/1538-4357/aab70c](https://doi.org/10.3847/1538-4357/aab70c)
- Michel, F. C. 1988, *Nature*, 333, 644, doi: [10.1038/333644a0](https://doi.org/10.1038/333644a0)
- Mineshige, S., Nomura, H., Hirose, M., Nomoto, K., & Suzuki, T. 1997, *ApJ*, 489, 227, doi: [10.1086/304776](https://doi.org/10.1086/304776)
- Ofengeim, D. D., & Gusakov, M. E. 2018, *PhRvD*, 98, 043007, doi: [10.1103/PhysRevD.98.043007](https://doi.org/10.1103/PhysRevD.98.043007)
- Parfrey, K., Spitkovsky, A., & Beloborodov, A. M. 2016, *ApJ*, 822, 33, doi: [10.3847/0004-637X/822/1/33](https://doi.org/10.3847/0004-637X/822/1/33)
- Passamonti, A., Akgün, T., Pons, J. A., & Miralles, J. A. 2017, *MNRAS*, 469, 4979, doi: [10.1093/mnras/stx1192](https://doi.org/10.1093/mnras/stx1192)
- Perna, R., Duffell, P., Cantiello, M., & MacFadyen, A. I. 2014, *ApJ*, 781, 119, doi: [10.1088/0004-637X/781/2/119](https://doi.org/10.1088/0004-637X/781/2/119)
- Philippov, A., Timokhin, A., & Spitkovsky, A. 2020, *PhRvL*, 124, 245101, doi: [10.1103/PhysRevLett.124.245101](https://doi.org/10.1103/PhysRevLett.124.245101)
- Piro, A. L., & Ott, C. D. 2011, *ApJ*, 736, 108, doi: [10.1088/0004-637X/736/2/108](https://doi.org/10.1088/0004-637X/736/2/108)
- Pons, J. A., & Geppert, U. 2007, *A&A*, 470, 303, doi: [10.1051/0004-6361:20077456](https://doi.org/10.1051/0004-6361:20077456)
- Pons, J. A., Miralles, J. A., & Geppert, U. 2009, *A&A*, 496, 207, doi: [10.1051/0004-6361:200811229](https://doi.org/10.1051/0004-6361:200811229)
- Pons, J. A., & Viganò, D. 2019, *Living Reviews in Computational Astrophysics*, 5, 3, doi: [10.1007/s41115-019-0006-7](https://doi.org/10.1007/s41115-019-0006-7)
- Pons, J. A., Viganò, D., & Rea, N. 2013, *Nature Physics*, 9, 431, doi: [10.1038/nphys2640](https://doi.org/10.1038/nphys2640)
- Poutanen, J., Lipunova, G., Fabrika, S., Butkevich, A. G., & Abolmasov, P. 2007, *MNRAS*, 377, 1187, doi: [10.1111/j.1365-2966.2007.11668.x](https://doi.org/10.1111/j.1365-2966.2007.11668.x)
- Rea, N., Borghese, A., Esposito, P., et al. 2016, *ApJL*, 828, L13, doi: [10.3847/2041-8205/828/1/L13](https://doi.org/10.3847/2041-8205/828/1/L13)

- Romanova, M. M., Ustyugova, G. V., Koldoba, A. V., & Lovelace, R. V. E. 2005, *ApJL*, 635, L165, doi: [10.1086/499560](https://doi.org/10.1086/499560)
- Ruderman, M. A., & Sutherland, P. G. 1975, *ApJ*, 196, 51, doi: [10.1086/153393](https://doi.org/10.1086/153393)
- Spitkovsky, A. 2006, *ApJL*, 648, L51, doi: [10.1086/507518](https://doi.org/10.1086/507518)
- Taam, R. E., & van den Heuvel, E. P. J. 1986, *ApJ*, 305, 235, doi: [10.1086/164243](https://doi.org/10.1086/164243)
- Tan, C. M., Bassa, C. G., Cooper, S., et al. 2018, *ApJ*, 866, 54, doi: [10.3847/1538-4357/aade88](https://doi.org/10.3847/1538-4357/aade88)
- Tingay, S. J., Goeke, R., Bowman, J. D., et al. 2013, *PASA*, 30, e007, doi: [10.1017/pasa.2012.007](https://doi.org/10.1017/pasa.2012.007)
- Ugliano, M., Janka, H.-T., Marek, A., & Arcones, A. 2012, *ApJ*, 757, 69, doi: [10.1088/0004-637X/757/1/69](https://doi.org/10.1088/0004-637X/757/1/69)
- van Haarlem, M. P., Wise, M. W., Gunst, A. W., et al. 2013, *A&A*, 556, A2, doi: [10.1051/0004-6361/201220873](https://doi.org/10.1051/0004-6361/201220873)
- Viganò, D., Garcia-Garcia, A., Pons, J. A., Dehman, C., & Graber, V. 2021, *Computer Physics Communications*, 265, 108001, doi: [10.1016/j.cpc.2021.108001](https://doi.org/10.1016/j.cpc.2021.108001)
- Viganò, D., Rea, N., Pons, J. A., et al. 2013, *MNRAS*, 434, 123, doi: [10.1093/mnras/stt1008](https://doi.org/10.1093/mnras/stt1008)
- Wang, Z., Chakrabarty, D., & Kaplan, D. L. 2006, *Nature*, 440, 772, doi: [10.1038/nature04669](https://doi.org/10.1038/nature04669)
- Wayth, R. B., Tingay, S. J., Trott, C. M., et al. 2018, *PASA*, 35, e033, doi: [10.1017/pasa.2018.37](https://doi.org/10.1017/pasa.2018.37)
- Wu, Q.-D., Zhi, Q.-J., Zhang, C.-M., Wang, D.-H., & Ye, C.-Q. 2020, *Research in Astronomy and Astrophysics*, 20, 188, doi: [10.1088/1674-4527/20/11/188](https://doi.org/10.1088/1674-4527/20/11/188)
- Yan, T., Perna, R., & Soria, R. 2012, *MNRAS*, 423, 2451, doi: [10.1111/j.1365-2966.2012.21051.x](https://doi.org/10.1111/j.1365-2966.2012.21051.x)
- Yao, J. M., Manchester, R. N., & Wang, N. 2017, *ApJ*, 835, 29, doi: [10.3847/1538-4357/835/1/29](https://doi.org/10.3847/1538-4357/835/1/29)
- Zanni, C., & Ferreira, J. 2013, *A&A*, 550, A99, doi: [10.1051/0004-6361/201220168](https://doi.org/10.1051/0004-6361/201220168)
- Zhong, Y., Kashiyama, K., Shigeyama, T., & Takasao, S. 2021, *ApJ*, 917, 71, doi: [10.3847/1538-4357/ac0a74](https://doi.org/10.3847/1538-4357/ac0a74)